

Bio-Lipid Nano Capacitors: Resonance with Helical Myeline Proteins

Majid Monajjemi ^{1*} , Farnoush Naghsh ², Fatemeh Mollaamin ¹

¹ Department of Chemical Engineering, Central Tehran Branch, Islamic Azad University, Tehran, Iran

² Department of Chemistry, Science and Research Branch, Islamic Azad University, Tehran, Iran

* Corresponding author e-mail address: maj.monajjemi@iauctb.ac.ir;

Scopus Author ID 6701810683

Received: 29.04.2020; Revised: 20.05.2020; Accepted: 22.05.2020; Published: 27.05.2020

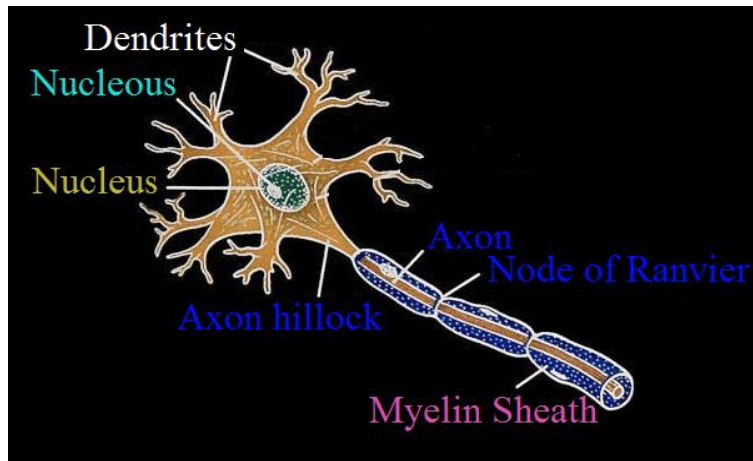
Abstract: The model of this work represents electrophysiological occurrences with a combination of some phospholipids such as POPC and galactocerebroside lipid bilayers as variable capacitors. The quantum effects of different thicknesses in the mixed membranes of GalC/POPC, GalC/ POPE, and GalC/DPPC have also explicitly been investigated. It is shown that quantum effects can appear in a small region of free spaces within the membrane thickness due to the number and type of lipid's layers. In the presence of external factors such as protein transmembrane and myelin proteins as a resistance, the forces can influence the state of the membrane, which results in a variable capacitance behavior. This allows introducing a capacitive susceptibility which can be resonating with the self-induction of helical coils in myelin proteins, the resonance of which is the main reason for various biological pulses.

Keywords: lipid bilayers; cell membrane capacitors; GaLC; POPC; DPPC; POPE; myelin-sheath.

© 2020 by the authors. This article is an open-access article distributed under the terms and conditions of the Creative Commons Attribution (CC BY) license (<https://creativecommons.org/licenses/by/4.0/>).

1. Introduction

Myelin consists of fatty molecules (lipids) which are located in the CNS (central nervous system) and as an insulator around nerve cell axons increases the velocities information to transit from one nerve cell to another tissue [1,2] like an electrical wire (the axon) with insulating material (myelin) around it [1]. In other words, reducing axonal membrane capacitance through insulating the axon increases the action potential due to large distances between the cations on the outside of the axon and Na^+ that move through the axonal cytoplasm (axoplasm) [3]. Since the length neither of NOR (around one micron) compares to adjacent long myelinated internodes (around one millimeter) is too much shorter (1000 times), suddenly an electrical signal in a critical point between insulated myelinated towards uninsulated of unmyelinated stimulates the release of a chemical message or neurotransmitter that binds to receptors on the adjacent post-synaptic cell at specified area called synapses [4,5]. The insulating structure for myelin is essential for hearing, seeing, feeling, the sensation of pain, and as well as perception, knowledge, and memory. Therefore, multiple sclerosis, which mainly affects the central nervous system, is related to the disordering of myelin [6,7]. The principal operation of myelin is providing acceleration to electrical impulses propagate along with the myelinated fiber [8]. Although in unmyelinated fibers, electrical impulses move as continuous waves, in myelinated fibers, they are propagated via saltatory conduction, which is faster than a continuous wave. Myelin reduces the capacitor capacitance, consequently enhances the electrical resistance across the axonal membrane (Scheme 1) [9-11].

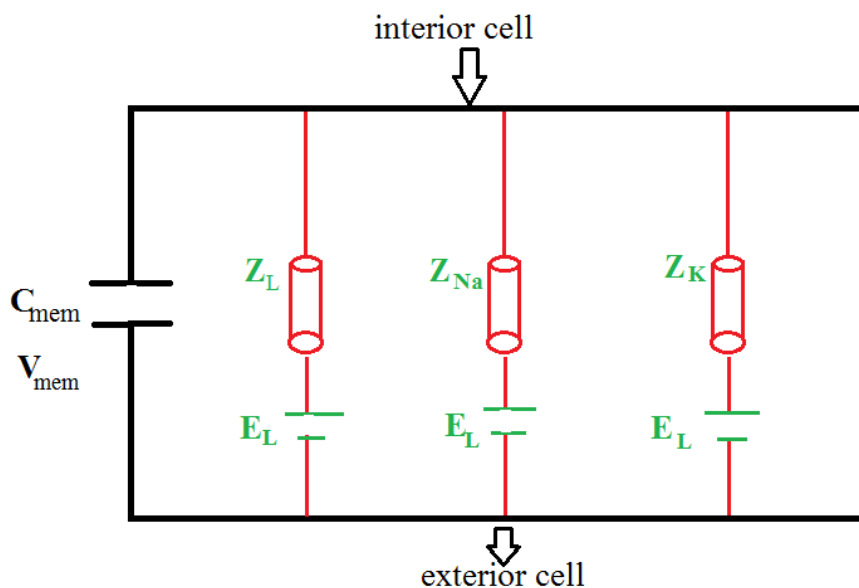


Scheme 1. A part of neuron, including myelin-sheath, Node of Ranvier, and neurofibrils.

Neurons transmit information by an electrical impulse that works as an action potential and has a velocity between 1 and 100 m/s. Neurons receive the pulses from dendrites and propagate the pulses with axon and connect to other cells via synapses electrically or sometimes chemically, therefore there are various neurons in the viewpoint of shapes, sizes, and electrochemical properties which generally contain a nucleus and organelles surrounded by membranes. The membranes are a combination of a lipid bilayer whose proteins are embedded inside glycolipids.

1.1. Electromechanical pulses.

In an ionic exchange, the net current could be separated into 1- fast inward current carried by Na^+ ions, and 2- slow activated outward current carried by K^+ ions, which are results from independent permeation mechanisms for sodium and potassium ions in the membrane. This approach is known as the ionic hypothesis (Scheme 2). Various ion currents contribute to the voltage signal of a neuron in which 3 of them are central, including sodium current, potassium current, leak current that consists (mostly chloride ions) that their flow is controlled via their respective voltage's channels in a membrane. The semipermeable membrane segregates the interior section from the exterior cell.



Scheme 2. A circuit of membranes including capacitor and ligands, sodium, and potassium channels as resistance.

I_{mem} is given by:

$$I_{mem}(t) = C_{mem} \frac{dV_{mem}}{dt} + Z_{Na}(V_{mem} - E_{Na}) + Z_K(V_{mem} - E_K) + Z_{Leak}(V_{mem} - E_{Leak})$$

where E_{Na} , E_K and E_{Leak} are the Nernst potentials of different ions. It also is given by equation $E_i = \frac{RT}{zF} \ln \frac{C_{out}}{C_{in}}$ where C_{out} and C_{in} are the concentrations of ions on the inner and outer side of the cell. This equation indicates that current flows due to diffusion along the gradients (even in the absence of other external voltages). Consequently, if the external voltage is equal to the Nernst potential, no current flows. Using Kirchhoff's laws, "cable".

1.2. Membrane contains POPC, GalC, POPE, and DPPC.

The cable equation of currents for potential propagation along GalC of myelinated axons yields a dynamics behavior. By this works, a small piece of cell membrane including pure GalC, POPC, DPPC, POPE, and also a mixing of GalC/DPPC, GalC/POPC and GalC/POPE with 50% mol ratio of each have been simulated for our model of membrane capacitors (Fig.1).

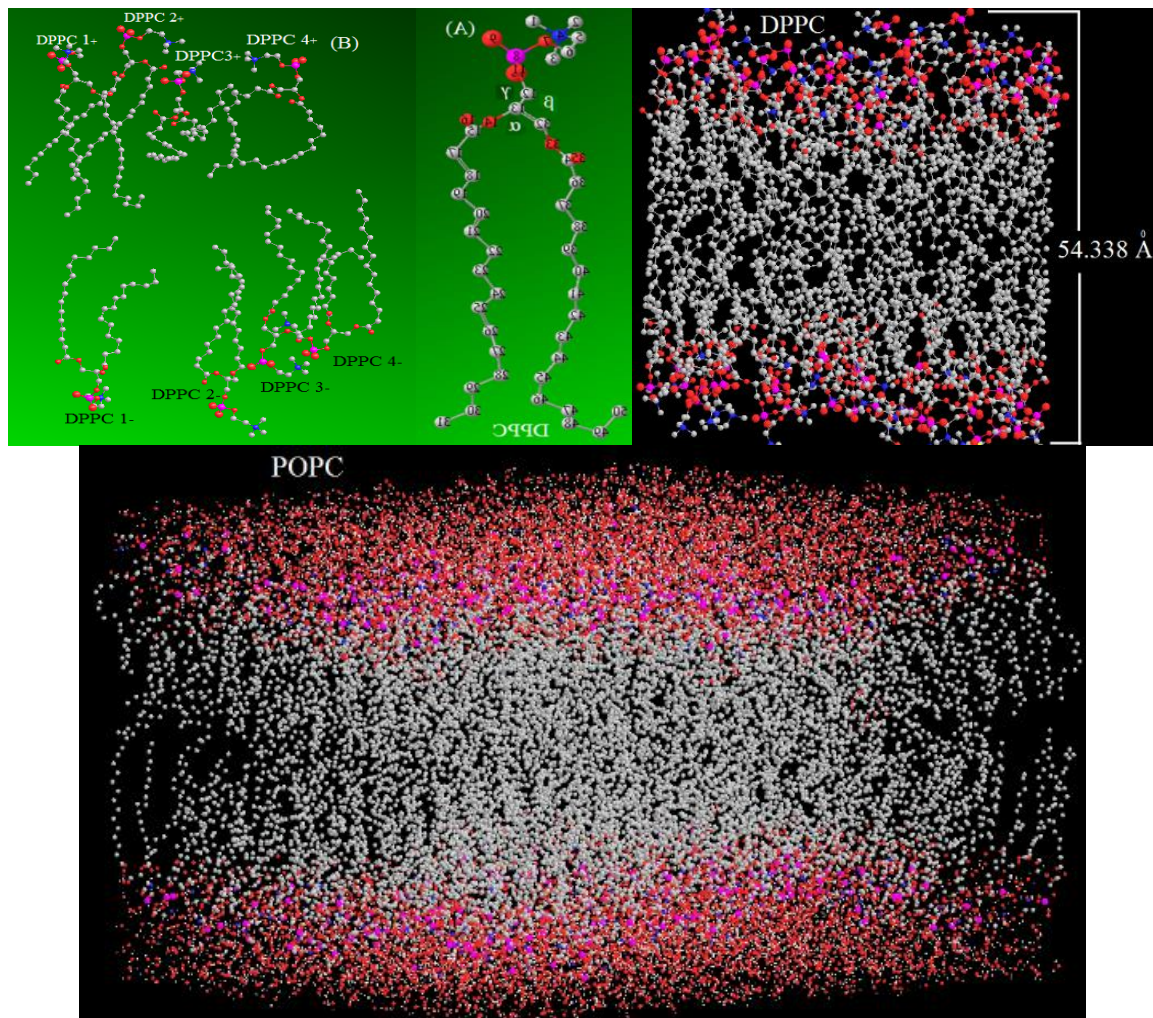
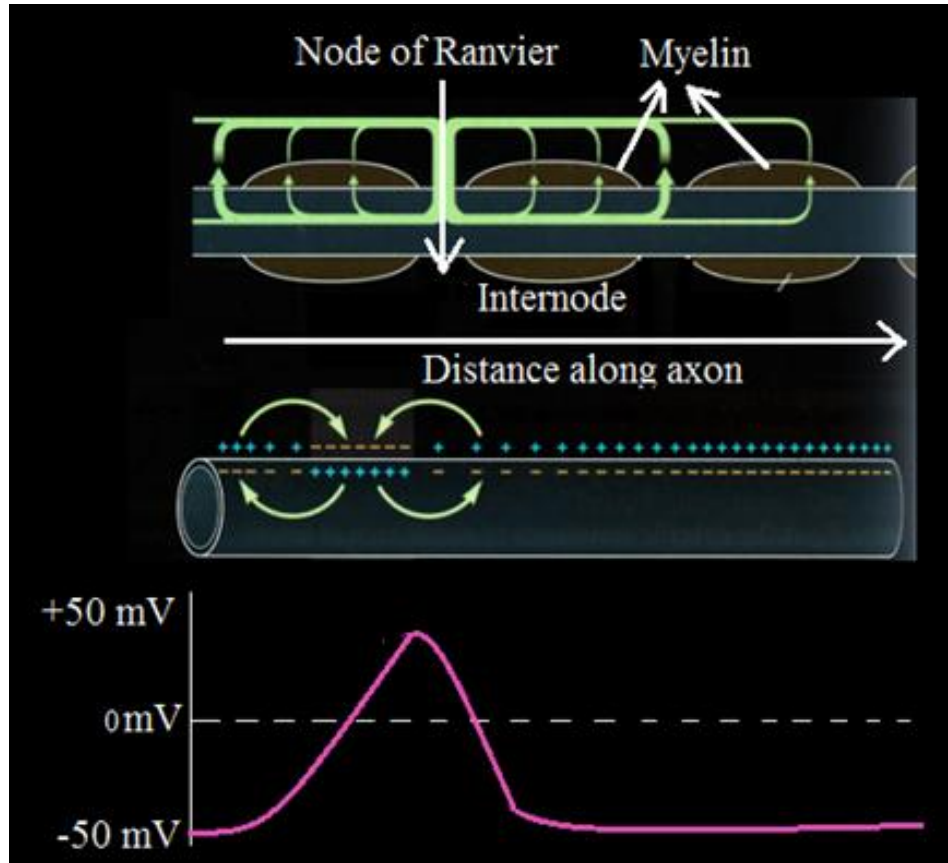


Figure 1. Monte Carlo calculation of various membranes including DPPC and POPC

1.3. Membrane capacitor model.

Capacitance can be calculated from the rate and amplitude changes in the voltage responses based on voltage clamp. These ways are applied widely to determine the total

capacitance of several neurons membrane. By this work, we simulated our systems based on several membrane thicknesses in the viewpoint of capacitors. In detail, Glial cell wraps around axons a few times (30-150 times) this like adding 330 membranes in the series. Therefore, through myelination, the diameter of the axon increases, and the speed of conduction increased by the diameter of the axon. Besides, potential action is related to $\frac{1}{r_a C_{membrane}}$ (scheme 3).



Scheme 3. Voltages are changing of myelin along the axon.

Generally, only two or three terms adequately describe $V_{mem}(t)$ (Fig.2). Through dividing "I_{ext}" to a series of the resistive terms as $R_i = \frac{V_i}{I_{ext}}$ steady-state can be evaluated as the sum of these resistive terms " $R_{in} = \frac{\Delta V_{mem}}{I_{ext}}$ ". The time constant of the slowest exponential ($e^{-t/\tau} = 0$) corresponds to the membrane time constant $\tau_m = r_m C_m$.

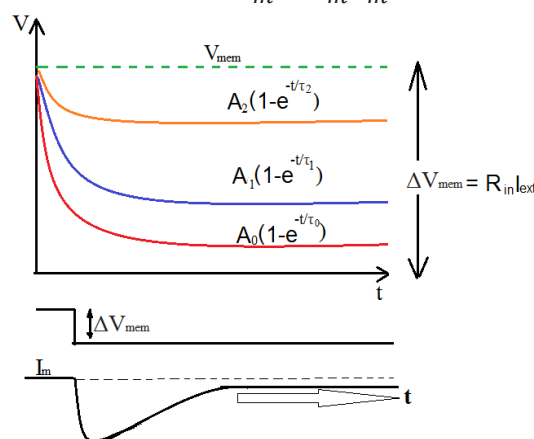


Figure 2. Schematic diagrams representing the membrane potential change, voltage-clamp step, and the charge deposited on the membrane for a given "V_{mem}".

It is also exhibited that the quantum effects are able to change the membrane's capacitances due to the external effects. Also, it is also concluded that the electrical properties of the membranes are affected via the application of electron densities in the membranes mentioned above. In our previous works, it has been declared [36-65] that the quantum components are a manifestation of the density of states (Dos) of the phosphate or galactose groups and their Thomas-Fermi screening lengths. Hence, the hybrid capacitance of any Nano-capacitor architecture is as follows:

$$C_{mem} = \left(\frac{1}{c_{mem}^{Qua}(one\ hand)} + \frac{1}{c_{mem}^{geo}} + \frac{1}{c_{mem}^{Qua}(opposite\ hand)} \right)^{-1} \text{ where } c_{mem}^{Qua}(top\ side)$$

and $c_{mem}^{Qua}(down\ side)$ are the quantum capacitances due to the finite Dos of the phosphate group's electrodes, respectively, as illustrated in Fig. 3.

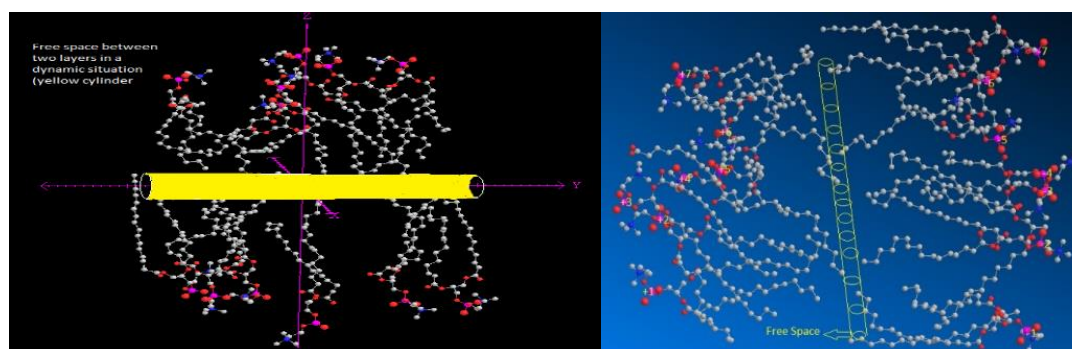


Figure 3. Quantum capacitances due to the finite Dos of the phosphate group's electrodes.

A change in voltage leads to a capacitive current due to the changes in the charge on the capacitor which is given by: $\frac{dQ}{dt} = \frac{d}{dt} [C_{mem} \cdot V_{mem}] = C_{mem} \frac{dV_{mem}}{dt} + V_{mem} \frac{dC_{mem}}{dt}$ and $\frac{dC_{mem}}{dt} = f \left(\frac{dC_{mem}^{geo}}{dt}, \frac{dC_{mem}^{qua}}{dt} \right)$. Heimburg exhibited that the changing voltages during the nerves pulses are entirely dependent on the capacitances changing. In addition, transition voltages can exchange the ions. They have also exhibited how the electrical properties of the membranes are affected through the application of lateral pressure or tension in a membrane. Consequently, It can be considered that any changing in the dimension of the membrane through electrical phenomenon depends on C_{mem}^{qua} (and independent to C_{mem}^{geo}), which means the tunneling effect is changing due to the dynamic system in the fluid mosaic model of the membrane.

2. Materials and Methods

2.1. Computational details.

The final parameterization of GalC/DPPC, GalC/POPC, and GalC/POPE were computed using self-consistent field calculations in order to find the optimal pre-geometries, as well as the total and partial charges of each side of membranes. DFT or density functional theories with the van der Waals interaction were applied to model the exchange-correlation energies of DPPC monomers. All optimization of monomer molecules of each membrane were

performed through Gaussian 09. The main focus in this study is to obtain the results from DFT methods such as m062x, m06-L, and m06 for the (Myelin's lipids molecules)_n {n=1-10}. The m062x, m06-L, and m06-HF are advanced and novel functional with a suitable correspondence in non-bonded calculations between GalC/DPPC, GalC/POPC and GalC/POPE monomers and are useful for determining the voltages in viewpoint of distance differences distance between two lateral in two sides of myelin's lipids. For non-covalent interactions between two layers of membranes, the B3LYP method is not suitable for describing van der Waals forces via medium-range interaction. Based on our previous works [12-69] our systems have been simulated.

3. Results and Discussion

We used model descriptive structures of several membranes including GalC/DPPC, GalC/POPC and GalC/POPE with the simplest consisting of two spheres attached to the related ends of a cable, which denote neuritis (l_{length} & $d_{diameter}$). We modeled variations in neuronal component size through changing l_{length} & $d_{diameter}$.

The fatty acid's chains layers give negative amplitude which decreases rapidly if the layers are uniform and less rapidly if the terminal methyl groups are localized near the center, in order to give a narrow area of lower electron densities. In this work, GalC/DPPC, GalC/POPC, and GalC/POPE were chosen as the mixed membranes capacitors since the alkyl groups are an excellent space-filling, similar to that of a biological system. Since the alkyl chains in those membranes have an ideal electrical insulator that might be polarized through applying the external electrical fields, the expected thickness of alkyl's layers between those membranes plates has been estimated, optimized and applied as an excellent model of dielectric constant for those capacitances calculations (Table 1).

Table 1. Dielectric constant, capacitance and the stability energies of various modeled membrane capacitors in various thicknesses for GalC/DPPC capacitor

GalC/DPPC & Number of atoms	$\Delta E_s (eV)$	$\frac{\Delta V = \Delta(\sum V_{P+}^{1toN} - \sum V_{P-}^{1toN})}{\Delta(\sum Q_{P+}^{1-N} - \sum Q_{P-}^{1-N})}$	Expectation of dielectric thickness	$C_g (F) \times 10^{20}$	Dielectric Constant	
(N=50)	0.0	-	-	-	-	
(N=100)	+0.30	3.5	1.12	39.33	2.1	7.23
(N=200)	+1.25	3.2	1.42	38.23	4.7	7.15
(N=400)	0.95	4.9	1.63	40.31	1.2	6.13
(N=500)	+0.65	5.4	1.65	39.01	1.4	5.82
(N=600)	0.45	5.6	1.85	39.44	1.3	5.39
(N=3000)	1.45	5.75	1.90	40.25	1.3	6.29

Similar as other capacitors, the an-isotropic attachment of alkyl groups allows the formation of several layered structures. Long-ranges interlayers interactions play a prevailing role in characterizing the electrical and mechanical properties of those systems and hence their efficiency in these models of capacitors. The ESP curve is drawn versus the number of lipids in where the minimum values of the ESP correspond to the odd numbers of lipids. However,

as for the even numbers, the ESP values are constant, indicating that the variable capacitances in those membranes are independent of the number of lipids. This means, what makes the cell membranes for acting as a model of variable capacitors do not related to the internal structures, though; they depend on the external cellular effects the same as electrical situations and any other pulses. The interaction energy between two sides of the membrane (P₊₃₀, P₋₃₀) of the electrodes) is also calculated based on. The dielectric permittivity as a function of capacitor sizes was calculated using QM/MM methods (Table 2).

Table 2. The dielectric and capacitance C_Q= quantum capacitance, C_g= geometry capacitance, and C_{net}= net capacitance, of modeled of GalC/DPPC capacitor in various thicknesses.

GalC/DPPC & Number of atoms	$C_Q(F) \times 10^{19} = \frac{\Delta q(Q + \frac{\Delta q}{2})}{\Delta E_S}$		$C_{net}(F) \times 10^{19} = \frac{C_g C_Q}{C_Q + 2C_g}$	
	ESP	Mulliken	ESP	Mulliken
(N=500)	1.45	1.55	1.30	1.25
(N=600)	1.15	1.38	1.03	0.97
(N=2000)	1.66	1.83	1.17	1.20
(N=3000)	1.43	1.56	0.99	0.99

The nano-capacitances of C_g, C_Q and C_{net} for GalC/DPPC, GalC/POPC, and GalC/POPE in different thickness of dielectrics are listed in table 2. Although the dielectric strength can be deduced from the bandgap of an alkyl space filler, the dielectric constant is directly calculated, which is much more accurate than the other ways. For large dielectric thicknesses, the classical capacitances of the "C_g ∝ 1/d" is conformable. This conformability is not valid for short distances due to the quantum effect; therefore the dielectric permittivity as a function of dielectric size has been defined through, C_Q(F) × 10²⁰ = $\frac{\Delta q(Q + \frac{\Delta q}{2})}{\Delta E_S}$ and C_{net}(F) × 10²⁰ = $\frac{C_g C_Q}{C_Q + 2C_g}$ (Fig.4).

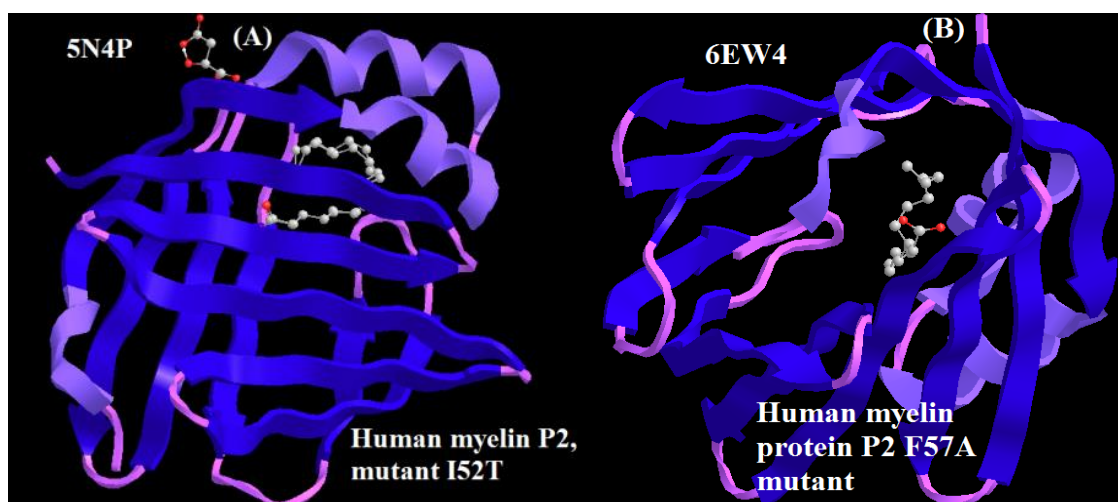


Figure 4. (A) Charcot-Marie-Tooth neuropathy linked to mutations in human myelin protein P2. (B) Structure of a human myelin protein P2, indicate the opening of the beta-barrel in fatty acid-binding proteins

4. Conclusions

It has been shown in this study that quantum effect has appeared in a small region of the membrane thickness due to the number of lipid bilayers. In the presence of external fields via protein trace membrane or channel ions, charges employ those forces that can influence the state of the membrane in myelin, thereby influencing the variable fields makes a variable

capacitance. This effect allows one to introduce a capacitive susceptibility that resonates with the self-induction effect of helical coils.

Funding

This research received no external funding.

Acknowledgments

We thank the central branch of IAU University due to provide software and main computers.

Conflicts of Interest

The authors declare no conflict of interest.

References

1. Keizer, J.; Smith, G.D.; Ponce-Dawson, S.; Pearson, J.E.; Saltatory propagation of Ca²⁺ waves by Ca²⁺ sparks. *Biophysical Journal* **1998**, *75*, 595–600, [https://doi.org/10.1016/S0006-3495\(98\)77550-2](https://doi.org/10.1016/S0006-3495(98)77550-2).
2. Boullerne, A.I. The history of myelin. *Exp Neurol* **2016**, *283*, 431–445, <https://doi.org/10.1016/j.expneurol.2016.06.005>.
3. Salzer, J.L. Clustering sodium channels at the node of Ranvier: close encounters of the axon-glia kind. *Neuron* **1997**, *18*, 843–846, [https://doi.org/10.1016/S0896-6273\(00\)80323-2](https://doi.org/10.1016/S0896-6273(00)80323-2).
4. Monajjemi, M. Cell membrane causes the lipid bilayers to behave as variable capacitors: A resonance with self-induction of helical proteins. *Biophysical Chemistry* **2015**, *207*, 114–127, <https://doi.org/10.1016/j.bpc.2015.10.003>.
5. Swire, M.; Ffrench-Constant, C. Seeing Is Believing: Myelin Dynamics in the Adult CNS. *Neuron* **2018**, *98*, 684–686, <https://doi.org/10.1016/j.neuron.2018.05.005>.
6. Hughes, E.G.; Orthmann-Murphy, J.L.; Langseth, A.J.; Bergles, D.E. Myelin remodeling through experience-dependent oligodendrogenesis in the adult somatosensory cortex. *Nature Neuroscience* **2018**, *21*, 696–706, <https://doi.org/10.1038/s41593-018-0121-5>.
7. Hartline, D.K. What is myelin? *Neuron Glia Biology* **2008**, *4*, 153–163, <https://doi.org/10.1017/S1740925X09990263>.
8. Salzer, J.L.; Zalc, B. Myelination. *Current Biology* **2016**, *26*, R971–R975, <https://doi.org/10.1016/j.cub.2016.07.074>.
9. Steinman, M.D. Multiple Sclerosis: A Coordinated Immunological Attack against Myelin in the Central Nervous System. *Cell* **1996**, *85*, 299–302, [https://doi.org/10.1016/S0092-8674\(00\)81107-1](https://doi.org/10.1016/S0092-8674(00)81107-1).
10. Greer, J.M.; Lees, M.B. Myelin proteolipid protein—the first 50 years. *The International Journal of Biochemistry & Cell Biology* **2002**, *34*, 211–215, [https://doi.org/10.1016/S1357-2725\(01\)00136-4](https://doi.org/10.1016/S1357-2725(01)00136-4).
11. Kaplan, M.R.; Cho, M.-H.; Ullian, E.M.; Isom, L.L.; Levinson, S.R.; Barres, B.A. Differential Control of Clustering of the Sodium Channels Nav1.2 and Nav1.6 at Developing CNS Nodes of Ranvier. *Neuron* **2001**, *30*, 105–119, [https://doi.org/10.1016/S0896-6273\(01\)00266-5](https://doi.org/10.1016/S0896-6273(01)00266-5).
12. Mollaamin, F.; Monajjemi, M. DFT outlook of solvent effect on function of nano bioorganic drugs. *Physics and Chemistry of Liquids* **2012**, *50*, 596–604, <https://doi.org/10.1080/00319104.2011.646444>.
13. Mollaamin, F.; Gharibe, S.; Monajjemi, M. Synthesis of various nano and micro ZnSe morphologies by using hydrothermal method. *International Journal of Physical Sciences* **2011**, *6*, 1496–1500.
14. Monajjemi, M. Graphene/(h-BN)_n/X-doped raphene as anode material in lithium ion batteries (X = Li, Be, B AND N). *Macedonian Journal of Chemistry and Chemical Engineering* **2017**, *36*, 101–118, <http://dx.doi.org/10.20450/mjcc.2017.1134>.
15. Monajjemi, M. Cell membrane causes the lipid bilayers to behave as variable capacitors: A resonance with self-induction of helical proteins. *Biophysical Chemistry* **2015**, *207*, 114–127, <https://doi.org/10.1016/j.bpc.2015.10.003>.
16. Monajjemi, M. Study of CD⁵⁺ Ions and Deuterated Variants (CH_xD(5-x)⁺): An Artefactual Rotation. *Russian Journal of Physical Chemistry A* **2018**, *92*, 2215–2226.
17. Monajjemi, M. Liquid-phase exfoliation (LPE) of graphite towards graphene: An ab initio study. *Journal of Molecular Liquids*, **2017**, *230*, 461–472, <https://doi.org/10.1016/j.molliq.2017.01.044>.
18. Jalilian, H.; Monajjemi, M. Capacitor simulation including of X-doped graphene (X = Li, Be, B) as two electrodes and (h-BN)_m (m = 1–4) as the insulator. *Japanese Journal of Applied Physics* **2015**, *54*, 085101–7.

19. Ardalan, T.; Ardalan, P.; Monajjemi, M. Nano theoretical study of a C 16 cluster as a novel material for vitamin C carrier. *Fullerenes Nanotubes and Carbon Nanostructures* **2014**, *22*, 687-708, <https://doi.org/10.1080/1536383X.2012.717561>.
20. Mahdavian, L.; Monajjemi, M.; Mangkorntong, N. Sensor response to alcohol and chemical mechanism of carbon nanotube gas sensors *Fullerenes Nanotubes and Carbon Nanostructures* **2009**, *17*, 484-495, <https://doi.org/10.1080/15363830903130044>.
21. Monajjemi, M.; Najafpour, J. Charge density discrepancy between NBO and QTAIM in single-wall armchair carbon nanotubes. *Fullerenes Nanotubes and Carbon Nano structures* **2014**, *22*, 575-594, <https://doi.org/10.1080/1536383X.2012.702161>.
22. Monajjemi, M.; Hosseini, M.S. Non bonded interaction of B16 N16 nano ring with copper cations in point of crystal fields. *Journal of Computational and Theoretical Nanoscience* **2013**, *10*, 2473- 2477
23. Monajjemi, M.; Mahdavian, L.; Mollaamin, F. Characterization of nanocrystalline silicon germanium film and nanotube in adsorption gas by Monte Carlo and Langevin dynamic simulation. *Bulletin of the Chemical Society of Ethiopia* **2008**, *22*, 277-286, <https://doi.org/10.4314/bcse.v22i2.61299>.
24. Lee, V.S.; Nimmanpipug, P.; Mollaamin, F.; Thanasanvorakun, S.; Monajjemi, M. Investigation of single wall carbon nanotubes electrical properties and normal mode analysis: Dielectric effects. *Russian Journal of Physical Chemistry A* **2009**, *83*, 2288-2296, <https://doi.org/10.1134/S0036024409130184>.
25. Mollaamin, F.; Najafpour, J.; Ghadami, S.; Akrami, M.S.; Monajjemi, M. The electromagnetic feature of B N H (x = 0, 4, 8, 12, 16, and 20) nano rings: Quantum theory of atoms in molecules/NMR approach. *Journal of Computational and Theoretical Nanoscience* **2014**, *11*, 1290-1298.
26. Monajjemi, M.; Mahdavian, L.; Mollaamin, F.; Honarparvar, B. Thermodynamic investigation of enolketo tautomerism for alcohol sensors based on carbon nanotubes as chemical sensors. *Fullerenes Nanotubes and Carbon Nanostructures* **2010**, *18*, 45-55, <https://doi.org/10.1080/15363830903291564>.
27. Monajjemi, M.; Ghiasi, R.; Seyed, S.M.A. Metal-stabilized rare tautomers: N4 metalated cytosine (M = Li , Na , K , Rb and Cs), theoretical views. *Applied Organometallic Chemistry* **2003**, *17*, 635-640, <https://doi.org/10.1002/aoc.469>.
28. Ilkhani, A.R.; Monajjemi, M. The pseudo Jahn-Teller effect of puckering in pentatomic unsaturated rings C AE , A=N, P, As, E=H, F, Cl. *Computational and Theoretical Chemistry* **2015**, *1074*, 19-25, <http://dx.doi.org/10.1016%2Fj.comptc.2015.10.006>.
29. Monajjemi, M. Non-covalent attraction of B N and repulsion of B N in the B N ring: a quantum rotatory due to an external field. *Theoretical Chemistry Accounts* **2015**, *134*, 1-22, <https://doi.org/10.1007/s00214-015-1668-9>.
30. Monajjemi, M.; Naderi, F.; Mollaamin, F.; Khaleghian, M. Drug design outlook by calculation of second virial coefficient as a nano study. *Journal of the Mexican Chemical Society* **2012**, *56*, 207-211, <https://doi.org/10.29356/jmcs.v56i2.323>.
31. Monajjemi, M.; Bagheri, S.; Moosavi, M.S. Symmetry breaking of B2N(-,0,+): An aspect of the electric potential and atomic charges. *Molecules* **2015**, *20*, 21636-21657, <https://doi.org/10.3390/molecules201219769>.
32. Monajjemi, M.; Mohammadian, N.T. S-NICS: An aromaticity criterion for nano molecules. *Journal of Computational and Theoretical Nanoscience* **2015**, *12*, 4895-4914, <https://doi.org/10.1166/jctn.2015.4458>.
33. Monajjemi, M.; Ketabi, S.; Hashemian, Z.M.; Amiri, A. Simulation of DNA bases in water: Comparison of the Monte Carlo algorithm with molecular mechanics force fields. *Biochemistry (Moscow)* **2006**, *71*, 1-8, <https://doi.org/10.1134/s0006297906130013>.
34. Monajjemi, M.; Lee, V.S.; Khaleghian, M.; Honarparvar, B.; Mollaamin, F. Theoretical Description of Electromagnetic Nonbonded Interactions of Radical, Cationic, and Anionic NH2BHNBNH2 Inside of the B18N18 Nanoring. *J. Phys. Chem C* **2010**, *114*, 15315-15330, <https://doi.org/10.1021/jp104274z>.
35. Monajjemi, M.; Boggs, J.E. A New Generation of BnNn Rings as a Supplement to Boron Nitride Tubes and Cages. *J. Phys. Chem. A* **2013**, *117*, 1670-1684, <http://dx.doi.org/10.1021/jp312073q>.
36. Monajjemi, M. Non bonded interaction between BnNn (stator) and BN B (rotor) systems: A quantum rotation in IR region. *Chemical Physics* **2013**, *425*, 29-45, <https://doi.org/10.1016/j.chemphys.2013.07.014>.
37. Monajjemi, M.; Robert, W.J.; Boggs, J.E. NMR contour maps as a new parameter of carboxyl's OH groups in amino acids recognition: A reason of tRNA-amino acid conjugation. *Chemical Physics* **2014**, *433*, 1-11, <https://doi.org/10.1016/j.chemphys.2014.01.017>.
38. Monajjemi, M. Quantum investigation of non-bonded interaction between the B15N15 ring and BH2NBH2 (radical, cation, and anion) systems: a nano molecular motor. *Struct Chem* **2012**, *23*, 551-580, <http://dx.doi.org/10.1007/s11224-011-9895-8>.
39. Monajjemi, M. Metal-doped graphene layers composed with boron nitride-graphene as an insulator: a nano-capacitor. *Journal of Molecular Modeling* **2014**, *20*, 2507, <https://doi.org/10.1007/s00894-014-2507-y>.
40. Mollaamin, F.; Monajjemi, M.; Mehrzad, J. Molecular Modeling Investigation of an Anti-cancer Agent Joint to SWCNT Using Theoretical Methods. *Fullerenes, Nanotubes and Carbon Nanostructures* **2014**, *22*, 738-751, <https://doi.org/10.1080/1536383X.2012.731582>.

41. Monajjemi, M.; Ketabi, S.; Amiri, A. Monte Carlo simulation study of melittin: protein folding and temperature dependence. *Russian journal of physical chemistry* **2006**, *80*, S55-S62, <https://doi.org/10.1134/S0036024406130103>.
42. Monajjemi, M.; Heshmata, M.; Haeria, H.H. QM/MM model study on properties and structure of some antibiotics in gas phase: Comparison of energy and NMR chemical shift. *Biochemistry (Moscow)* **2006**, *71*, S113-S122, <https://doi.org/10.1134/S0006297906130190>.
43. Monajjemi, M.; Afsharnezhad, S.; Jaafari, M.R.; Abdolahi, T.; Nikosade, A.; Monajemi, H. NMR shielding and a thermodynamic study of the effect of environmental exposure to petrochemical solvent on DPPC, an important component of lung surfactant. *Russian Journal of Physical Chemistry A* **2007**, *81*, 1956-1963, <https://doi.org/10.1134/S0036024407120096>.
44. Mollaamin, F.; Noei, M.; Monajjemi, M.; Rasoolzadeh, R. Nano theoretical studies of fMET-tRNA structure in protein synthesis of prokaryotes and its comparison with the structure of fALA-tRNA. *African journal of microbiology research* **2011**, *5*, 2667-2674, <https://doi.org/10.5897/AJMR11.310>.
45. Monajjemi, M.; Heshmat, M.; Haeri, H.H.; Kaveh, F. Theoretical study of vitamin properties from combined QM-MM methods: Comparison of chemical shifts and energy. *Russian Journal of Physical Chemistry* **2006**, *80*, 1061-1068, <https://doi.org/10.1134/S0036024406070119>.
46. Monajjemi, M.; Chahkandi, B. Theoretical investigation of hydrogen bonding in Watson–Crick, Hoogsteen and their reversed and other models: comparison and analysis for configurations of adenine–thymine base pairs in 9 models. *Journal of Molecular Structure: THEOCHEM* **2005**, *714*, 43-60, <https://doi.org/10.1016/j.theochem.2004.09.048>.
47. Monajjemi, M.; Honarparvar, B.; Haeri, H.H.; Heshmat, M. An ab initio quantum chemical investigation of solvent-induced effect on ¹⁴N-NQR parameters of alanine, glycine, valine, and serine using a polarizable continuum model. *Russian Journal of Physical Chemistry* **2006**, *80*, S40-S44, <https://doi.org/10.1134/S0036024406130073>.
48. Monajjemi, M.; Seyed Hosseini, M. Non Bonded Interaction of B16N16 Nano Ring with Copper Cations in Point of Crystal Fields. *Journal of Computational and Theoretical Nanoscience* **2013**, *10*, 2473-2477, <https://doi.org/10.1166/jctn.2013.3233>.
49. Monajjemi, M.; Farahani, N.; Mollaamin, F. Thermodynamic study of solvent effects on nanostructures: phosphatidylserine and phosphatidylinositol membranes. *Physics and Chemistry of Liquids* **2012**, *50*, 161-172, <https://doi.org/10.1080/00319104.2010.527842>.
50. Monajjemi, M.; Ahmadianarog, M. Carbon Nanotube as a Deliver for Sulforaphane in Broccoli Vegetable in Point of Nuclear Magnetic Resonance and Natural Bond Orbital Specifications. *Journal of Computational and Theoretical Nanoscience* **2014**, *11*, 1465-1471, <https://doi.org/10.1166/jctn.2014.3519>.
51. Monajjemi, M.; Ghiasi, R.; Ketabi, S.; Passdar, H.; Mollaamin, F. A Theoretical Study of Metal-Stabilised Rare Tautomers Stability: N4 Metalated Cytosine (M=Be²⁺, Mg²⁺, Ca²⁺, Sr²⁺ and Ba²⁺) in Gas Phase and Different. *Journal of Chemical Research* **2004**, *1*, 11-18, <https://doi.org/10.3184/030823404323000648>.
52. Monajjemi, M.; Baei, M.T.; Mollaamin, F. Quantum mechanic study of hydrogen chemisorptions on nanocluster vanadium surface. *Russian Journal of Inorganic Chemistry* **2008**, *53*, 1430-1437, <https://doi.org/10.1134/S0036023608090143>.
53. Mollaamin, F.; Baei, M.T.; Monajjemi, M.; Zhiani, R.; Honarparvar, B. A DFT study of hydrogen chemisorption on V (100) surfaces. *Russian Journal of Physical Chemistry A, Focus on Chemistry* **2008**, *82*, 2354-2361, <https://doi.org/10.1134/S0036024408130323>.
54. Monajjemi, M.; Honarparvar, B.; Nasser, S.M.; Khaleghian, M. NQR and NMR study of hydrogen bonding interactions in anhydrous and monohydrated guanine cluster model: A computational study. *Journal of Structural Chemistry* **2009**, *50*, 67-77, <https://doi.org/10.1007/s10947-009-0009-z>.
55. Monajjemi, M.; Aghaie, H.; Naderi, F. Thermodynamic study of interaction of TSPP, CoTsPc, and FeTsPc with calf thymus DNA. *Biochemistry (Moscow)* **2007**, *72*, 652-657, <https://doi.org/10.1134/S0006297907060089>.
56. Monajjemi, M.; Heshmat, M.; Aghaei, H.; Ahmadi, R.; Zare, K. Solvent effect on ¹⁴N NMR shielding of glycine, serine, leucine, and threonine: Comparison between chemical shifts and energy versus dielectric constant. *Bulletin of the Chemical Society of Ethiopia* **2007**, *21*, 111-116, <https://doi.org/10.4314/bcse.v21i1.61387>.
57. Monajjemi, M.; Rajaeian, E.; Mollaamin, F.; Naderi, F.; Saki, S. Investigation of NMR shielding tensors in 1,3 dipolar cycloadditions: solvents dielectric effect. *Physics and Chemistry of Liquids* **2008**, *46*, 299-306, <https://doi.org/10.1080/00319100601124369>.
58. Mollaamin, F.; Varmaghani, Z.; Monajjemi, M. Dielectric effect on thermodynamic properties in vinblastine by DFT/Onsager modelling. *Physics and Chemistry of Liquids* **2011**, *49*, 318-336, <https://doi.org/10.1080/00319100903456121>.
59. Monajjemi, M.; Honarparvar, B.; Khalili Hadad, B.; Ilkhani, A.; Mollaamin, F. Thermo-Chemical Investigation and NBO Analysis of Some anxiolytic as Nano- Drugs. *African journal of pharmacy and pharmacology* **2010**, *4*, 521-529.

60. Monajjemi, M.; Khaleghian, M.; Mollaamin, F. Theoretical study of the intermolecular potential energy and second virial coefficient in the mixtures of CH₄ and Kr gases: a comparison with experimental data. *Molecular Simulation* **2010**, *36*, 865-870, <https://doi.org/10.1080/08927022.2010.489557>.
61. Monajjemi, M.; Khosravi, M.; Honarparvar, B.; Mollaamin, F. Substituent and solvent effects on the structural bioactivity and anticancer characteristic of catechin as a bioactive constituent of green tea. *International Journal of Quantum Chemistry* **2011**, *111*, 2771-2777, <https://doi.org/10.1002/qua.22612>.
62. Tahan, A.; Monajjemi, M. Solvent dielectric effect and side chain mutation on the structural stability of Burkholderia cepacia lipase active site: a quantum mechanical/molecular mechanics study. *Acta Biotheor* **2011**, *59*, 291-312, <https://doi.org/10.1007/s10441-011-9137-x>.
63. Monajjemi, M.; Khaleghian, M. EPR Study of Electronic Structure of [CoF₆]³⁻ and B18N18 Nano Ring Field Effects on Octahedral Complex. *Journal of Cluster Science* **2011**, *22*, 673-692, <https://doi.org/10.1007/s10876-011-0414-2>.
64. Monajjemi, M.; Mollaamin, F. Molecular Modeling Study of Drug-DNA Combined to Single Walled Carbon Nanotube. *Journal of Cluster Science* **2012**, *23*, 259-272, <https://doi.org/10.1007/s10876-011-0426-y>.
65. Mollaamin, F.; Monajjemi, M. Fractal Dimension on Carbon Nanotube-Polymer Composite Materials Using Percolation Theory. *Journal of Computational and Theoretical Nanoscience* **2012**, *9*, 597-601, <https://doi.org/10.1166/jctn.2012.2067>.
66. Mahdavian, L.; Monajjemi, M. Alcohol sensors based on SWNT as chemical sensors: Monte Carlo and Langevin dynamics simulation. *Microelectronics Journal* **2010**, *41*, 142-149, <https://doi.org/10.1016/j.mejo.2010.01.011>.
67. Monajjemi, M.; Falahati, M.; Mollaamin, F. Computational investigation on alcohol nanosensors in combination with carbon nanotube: a Monte Carlo and ab initio simulation. *Ionics* **2013**, *19*, 155-164, <https://doi.org/10.1007/s11581-012-0708-x>.
68. Monajjemi, M. Molecular vibration of dopamine neurotransmitter: a relation between its normal modes and harmonic notes. *Biointerface Research in Applied Chemistry*, **2019**, *9*, 3956-3962, <https://doi.org/10.33263/BRIAC93.956962>.
69. Mollaamin, F.; Naiemi, M.; Monajjemi, M.; Vinblastine and vincristine as anticancer molecules stopping the tubulin dimers, *Letters in applied nano bio sciences*, **2019**, *9*, 870-874, <https://doi.org/10.33263/LIANBS91.870874>.